

## Transient Phenomena Analysis in Hydroelectric Power Plants at Off-Design Operating Conditions

Viktor Iliev, Predrag Popovski, Zoran Markov

"Ss. Cyril and Methodius" University, Faculty of Mechanical Engineering – Skopje, Macedonia

### ABSTRACT

The numerical and experimental investigation of the transient phenomena in hydroelectric power plants (HPPs) during off-design operating conditions is presented in this paper. Modeling of pipes, valves, surge tanks, Francis turbine and its draft tube based on one-dimensional approach is performed. Numerical simulation of transient phenomena is performed for different configuration of hydroelectric power plant at off-design conditions such as load rejection/emergency shut-down. Also, analysis of transient phenomena, such as increase of the rotational speed (runaway) of the units, increase of the pressure (head) in the hydraulic system (water hammer) and turbine draft tube pressure pulsations is calculated. Finally, numerical model of hydroelectric power plant, validated with existing measurements data, is used for investigation of influential criteria on HPP's guaranteed control values (allowed values of runaway, water hammer and minimum closing time of the guide vanes).

**Key words:** hydroelectric power plant, off-design, transient phenomena, runaway, water hammer, numerical simulation.

### I. INTRODUCTION

Hydroelectric power plant has an important role to play in stabilizing the electrical power grids. In the unstable (unregulated) electricity market, hydropower plants play an extremely important role in order to adapt the production to the demand of energy and therefore, units (turbine+generator) are more often working at maximum power, load changes and increasing number of startup and shutdown sequences. In addition, hydropower plants are constantly modernized to increase their flexibility by taking advantage of new control strategies.

Transient phenomena in HPPs occurs during unit shutdown or startup, switching from one operation regime of HPP to another, load rejection, emergency shutdown, out of phase of synchronization etc. All the above listed events induce changes of discharge, pressure, rotational speed, voltage, current and other flow and electricity values of the power plant. The accurate definition of the transient phenomena of the HPP and its units, taking into account various aspects of operation is an

essential requirement for the design, performances and control of HPPs.

This paper focuses on analysis of the unit dynamics and hydraulic components of a HPP, the so-called guarantee control values. In particular, the allowed increase of the rotational speed (runaway), the allowed increase of the pressure (water hammer) and pressure pulsations generated in the turbine draft tube. The case study of HPP operation presented here investigates different configuration of HPPs and transient scenarios. Numerical computation of the transient phenomena the HPPs is performed using commercial software package. Finally, numerical model of HPP, validated with existing measurements data, is used for investigation of influential criteria on HPP guarantee control values (allowed values of runaway and water hammer and minimum closing time of the guide vanes).

### II. MODELING OF THE HYDRAULIC COMPONENTS

The mathematical (numerical) models of the following basic components of hydroelectric power plant are presented here in more detail:

- pipe
- valve
- surge tank
- Francis turbine and
- turbine draft tube

#### II.1. Pipe model

Mathematical model for unsteady flow in pipes is obtained using a one-dimensional approach of modeling with conservation of matter law (continuity equation (eq.1)) and momentum (motion equation (eq.2)). In accordance with conservation of matter law, the continuity equation set for elementary particle in hydraulic pipes (Fig.1), after linearization, is obtained in the form [1]:

$$\frac{\partial H}{\partial t} + \frac{a^2}{gA} \frac{\partial Q}{\partial x} = 0; \quad (1)$$

Application of Newton's second law of motion to case of unsteady flow in and pipe (Fig.1) leads to motion equation [1]:

$$\frac{\partial H}{\partial x} + \frac{1}{gA} \frac{\partial Q}{\partial t} + \frac{\lambda Q|Q|}{2gDA^2} = 0; \quad (2)$$

The hyperbolic set of equation (1) and (2) with given initial and boundary conditions, can be solved numerically, often using a finite differences method (characteristics method) [2].

Pressure wave speed through the hydraulic system is calculated according to following equation, [2]:

$$a = \sqrt{\frac{1}{\rho \left( \frac{1}{K} + \frac{D}{\delta E} \right)}} \quad (3)$$

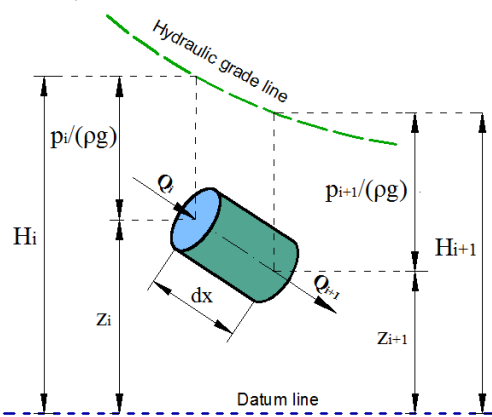


Fig.1. Elementary particle of hydraulic pipe with length  $dx$

## II.2. Valve model

The discharge of a valve at steady state conditions is [3]:

$$Q_0 = (c_Q)_0 \cdot A \cdot \sqrt{2gH_0} \quad (4)$$

where  $c_Q$  is valve discharge coefficient.

The valve discharge coefficient depending on valve characteristics (Fig.2) i.e. valve opening/closing law  $\tau(t)$  [3]:

$$c_Q(t) = \tau(t) \cdot (c_Q)_0 \quad (5)$$

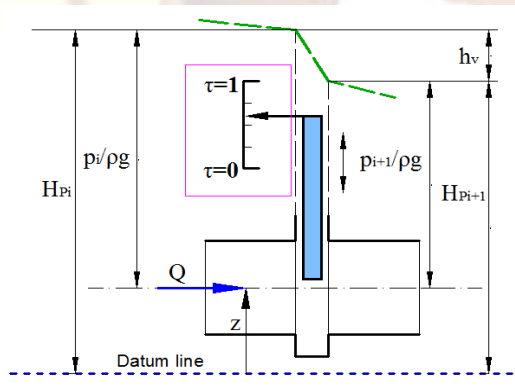


Fig. 2. Valve model

The discharge of a valve at unsteady state conditions is given with following equation [3]:

$$Q_v = c_{Q(t)} A_{(t)} \sqrt{2gH} \quad (6)$$

The discharge equation of a valve can be expressed as [3]:

$$h_v = \frac{Q_v |Q_v|}{c_{Q(t)}^2 2gH_0 A_{(t)}^2} \quad (7)$$

where  $A_{(t)}$  is the area of opening depending on  $\tau_{(t)}$ .

## II.3. Surge tank model

Surge tank dynamic model describes the inlet head losses and water level oscillations (the

amplitude  $Z$  and the period  $T$ ). In this research, a throttled surge tank is used (Fig. 3).

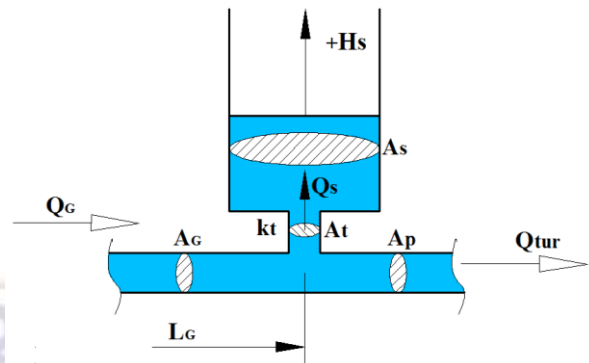


Fig. 3. Throttled surge tank model

Dynamic equations for surge tank are presented with the following equations [4]:

$$\frac{dQ_G}{dt} = \frac{gA_G}{L_G} (-H_S - k_{Q_G} |Q_G| - k_{t} Q_s |Q_s|) \quad \text{and} \quad (8)$$

$$\frac{dH_S}{dt} = \frac{1}{A_s} (Q_G - Q_{tur})$$

$$T = 2\pi \sqrt{\frac{LA_t}{gA_G}}; \quad \text{and} \quad Z = Q_{tur} \sqrt{\frac{L}{gA_t A_G}} \quad (9)$$

## II.4. Francis turbine model

Transient regimes in the electric power system initiate unbalanced torque between turbine and generator, thereby increasing the rotating speed, changes according to the angular momentum equation for the rotating mass according to the following equation [5]:

$$M_H - M_S = J \cdot \frac{d\omega}{dt}; \quad (10)$$

After a full load rejection conditions the electromagnetic resistance torque  $M_s$ , can be set equal to zero. According to equation (10), the mechanical inertia of unit  $J$  (turbine+generator) has a significant influence on the speed variation of the rotating mass of the unit. For unit with low mechanical inertia the runner speed increase rapidly after a full load rejection.

The influence of the turbine's water passage (Fig.4) on the hydraulic system can be defined by one-dimensional approach for modeling of the pipeline through the continuity and motion equation. The head (pressure) pulsations in hydraulic installation from the turbine are represented as [6]:

$$\Delta H = 2 \left[ \frac{1}{k_Q^2 D^4 g} \right] Q_2 |Q_1| - \left[ \frac{1}{k_Q^2 D^4 g} \right] Q_1 |Q_1|; \quad (11)$$

where:  $\Delta H$  is the head fluctuations between two point of computation,  $k_Q$  is discharge turbine coefficient computed from turbine characteristics (Fig.14) and expressed as function of guide vane opening and discharge value,  $Q_1$  and  $Q_2$  are the discharge values in the previous step from the computation and current discharge,  $D$  is the turbine runner diameter.

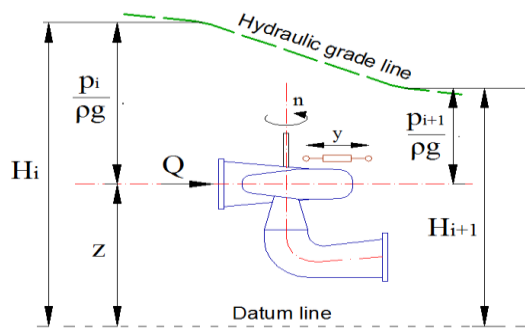


Fig. 4. Francis turbine model

The characteristic of the turbine can be defined as function of guide vane opening position  $a_0$  and the speed factor  $n_{11}$ , discharge factor  $Q_{11}$  and torque factor  $M_{11}$  [5]:

$$n_{11} = \frac{nD}{\sqrt{H}}; \quad Q_{11} = \frac{Q}{D^2\sqrt{H}}; \quad \text{and} \\ M_{11} = \frac{30\rho g Q_{11} \eta_T}{n_{11} \pi} \quad (12)$$

### II.5. Turbine draft tube model

The turbine draft tube is an important part of the turbine and it converts the kinetic energy at the runner exit into potential energy and therefore enables increasing the efficiency of the turbine (increasing the head of the runner). One of the major of the difficulties in the turbine is the existence of a vortex rope (gaseous volume) in the draft tube at off-design operating conditions. The vortex rope produces undesirable, periodic pressure pulsations (pressure surges) within the draft tube. These pressure pulsations produce existing forces that can affect components of the all systems of a hydroelectric power plant.

Using one-dimensional approach can be defined the turbine draft tube model (Fig.5) by modeling of the pipe with a pressure source excitation in series with two pipes that requires the length and cross section of the pipe obtained from the draft tube geometry and the wave speed, as input parameters. Modeling of the vortex rope gaseous volume is based on the assumption that the gaseous volume  $V$  depends of the state variables  $H$  (the net head) and  $Q$  (the discharge). The rate of change of the gaseous volume is given by the variation of discharge between the 2 fluid sections limiting the rope (Fig.6), [6,7,8]:

$$\frac{dV}{dt} = Q_1 - Q_2 = C \frac{dH_2}{dt} + \chi \frac{dQ_2}{dt}; \quad (13)$$

where:  $C = -\partial V / \partial H$  is cavity compliance and  $\chi = -\partial V / \partial Q_2$  is mass flow gain factor. Inertia and friction loss effects of the gas volume are negligible, i.e.  $H_2 = H_1$ .

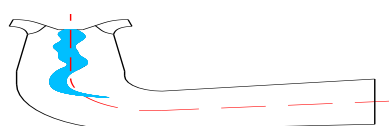


Fig. 5. Turbine draft tube model

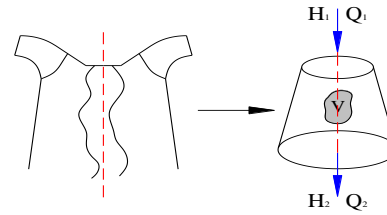


Fig. 6. The vortex rope gaseous volume, [7,8]

### III. CASE STUDIES

In this paper, numerical simulation and analysis of the transient phenomena are performed for hydroelectric power plant with different hydraulic configuration during off-design operation conditions. The software package WHAMO is used for all numerical computations.

#### III.1. Case study A: Elementary plant

In his case study the main aim is to analyze the occurrence of water hammer in, so called "elementary plant" consisting of reservoir-penstock-valve only, shown on Fig.7.

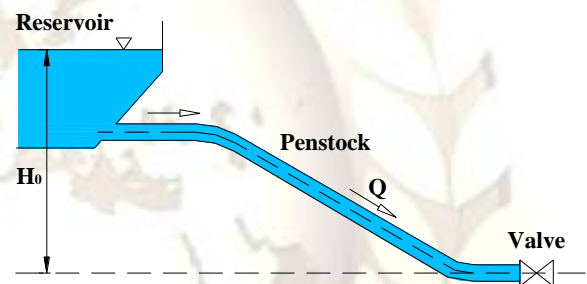


Fig. 7. Case study A: Reservoir-penstock-valve system

Configuration of hydraulic system is shown in table 1. The penstock is made of steel and accordingly, the pressure wave speed calculated using equation (3) is 1219 [m/s]. Valve closing time law presented in Fig.8 is given with the following equation [9]:

$$\tau(t) = 1 - \left( \frac{t - t_s}{t_c} \right)^{0.75} \quad (14)$$

where  $t_s$  represents time at the start of the valve closure, while  $t_c$  is valve closure time.

Table 1. System configuration for case study A.

Reservoir	Penstock	Valve
$H_0 = 150$ [m]	$L = 660$ [m]	$D_v = 0.6$ [m]
	$D = 0.6$ [m]	$(C_0)_0 = 0.0465$
	$\lambda = 0.03$	$Q_0 = 0.47$ [m <sup>3</sup> /s]
	$a = 1219$ [m/s]	$t_s = 1$ [s]
		$t_c = 3.5$ [s]



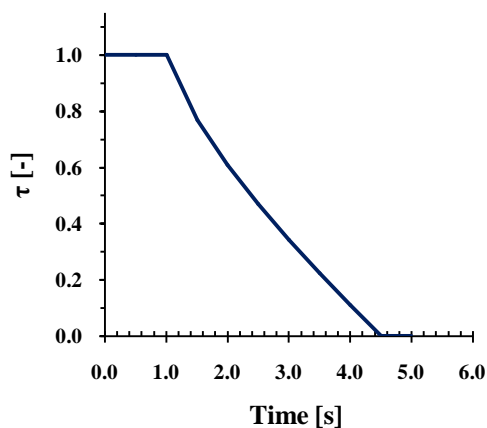


Fig. 8. Valve closing time law

Valve discharge coefficient (according eq.5) depending on closing time law is given in Fig.9 and pressure losses in the valve are defined according (eq. (7)).

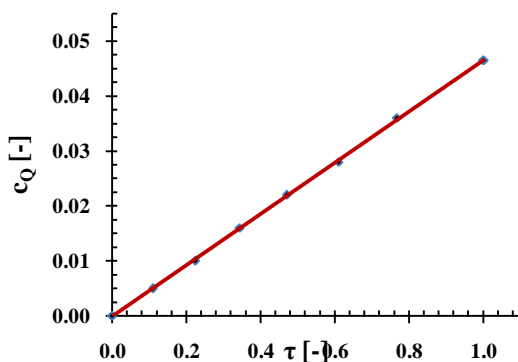


Fig. 9. Valve discharge coefficient

The minimum time step  $\Delta t$  needs to be determined for the iterative computation purposes. This time step is determined from the condition of complying with the Lewy-Courant criteria [10], that is  $Cr < 1$ :

$$\Delta t < L/(a \cdot n) = 660/(1219 \cdot 100) = 0.005 \text{ [sec]} \quad (15)$$

$Cr$  number must be less than 1:

$$Cr = a \cdot \Delta t / \Delta x = 1219 \cdot 0.005 / 6.6 = 0.93 < 1 \quad (16)$$

where  $n$  represents the number of segments that penstock is divided in, while  $\Delta x$  is the length of one segment.

The simulation parameters are summarized in table 2.

Table 2. Simulation parameters

n [-]	$\Delta t$ [sec]	$t_c$ [sec]	a [m/s]	$C_r$ [-]
100	0.001	3.5 [sec]	1219	0.2

Results of the numerical computation for valve closing time law according Fig.8 are given on Fig.10.

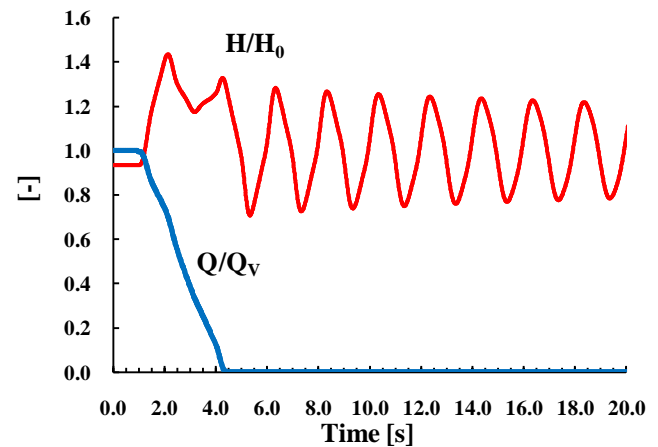


Fig. 10. Time evolution of the head  $H/H_0$  (water hammer) and the discharge at the valve  $Q/Q_V$

The computations show that the maximum pressure (water hammer) occurs at time  $t_s + 2L/a$  with a value of  $H_{\max}(\tau) = 1.45H_0$ , while minimum pressure value at the valve is  $H_{\min}(\tau) = 0.71H_0$ .

### III.2. Case study B: Hydroelectric power plant without surge tank

This case study analyses a model of hydropower plant consisting of upstream (intake) reservoir, penstock, valve, unit (150 MW vertical Francis turbine and generator) and downstream reservoir (tailrace) (Fig.11). The characteristics of the HPP are presented in table 3.

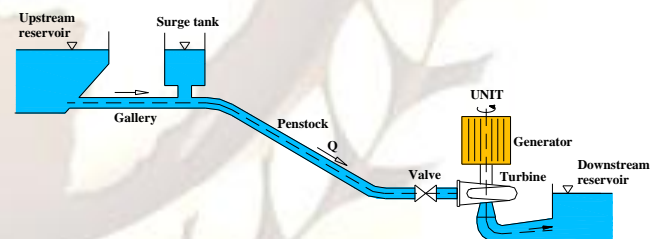


Fig. 11. Layout of the HPP (Case study B)

The transient phenomena of the power plant can be simulated for scenario with load rejection of the unit. The minimum time step of the iterations is calculated according eq.15. The guide vanes closing law ( $y$ ) after load rejection is shown in Fig. 12. The results of the numerical simulation and experimental data [11], are presented in Fig.12 (water hammer) and Fig.13 (runaway), using non-dimensional characteristics:

Table 3. Characteristics of HPP (rated values-Case

Upstream reservoir	Penstock	Francis turbine	Mechanical inertia of unit
$H_0=133$ [m]	$L = 1430$ [m] $D = 6$ [m] $\lambda = 0.024$ $a=1390$ [m/s]	$H_R = 126$ [m] $n_R = 200$ [min <sup>-1</sup> ] $Q_R = 136$ [m <sup>3</sup> /s] $M_R = 7.16e6$ [Nm]	Generator $J_G=26.5e6$ [kgm <sup>2</sup> ] Turbine $J_{TR}=9.14e4$ [kgm <sup>2</sup> ]

study B)

$\alpha = n/n_R$ ;  $h = h/h_R$ ;  $y = a_0/a_{Rmax}$   
where  $n_R$ ,  $H_R$  and  $a_{Rmax}$  are rated values for rotational speed, head at the inlet of turbine and guide vane opening value.

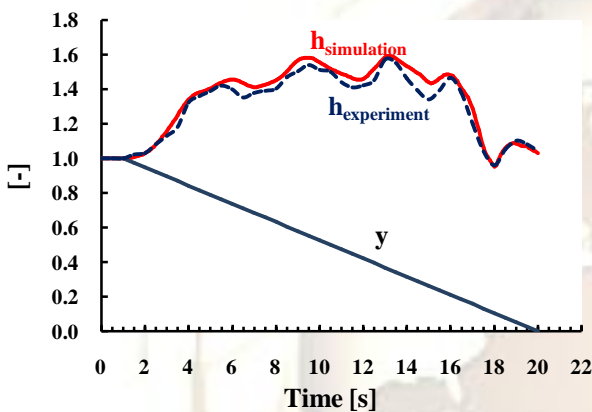


Fig.12. Results of the computation and experimental data for h (water hammer), and guide vanes closing law (y) (Case B)

Table 4. Characteristics of HPP (rated values-Case study C)

Upstream reservoir	Gallery	Surge tank	Penstock	Turbine	Turbine draft tube	Generator
$H_{0max}=109$ [m]	$L=98$ [m] $D=5.0$ [m] $\lambda=0.02$ $a=1050$ [m/s]	$A_S = 19.60$ [m <sup>2</sup> ] $A_t = 8.80$ [m <sup>2</sup> ] $H_{Smax}=40$ [m]	$L = 220$ [m] $D=5.0/3.12$ [m] $\lambda=0.02$ $a=1020$ [m/s]	$H_R=92$ [m] $n_R=300$ [min <sup>-1</sup> ] $Q_R=50$ [m <sup>3</sup> /s] $P_R=40$ [MW] $J_R = 30$ [tm <sup>2</sup> ]	$A_{inlet}=5.48$ [m <sup>2</sup> ] $A_{outlet}=20.3$ [m <sup>2</sup> ] $L_{DT} = 11$ [m] $a=700$ [m/s]	$J_G=1500$ tm <sup>2</sup>

The operating point trajectory in the plan (hill chart turbine diagram)  $Q_{11}(n_{11})$  during the load rejection for simulation and experimental are shown in Fig. 14.

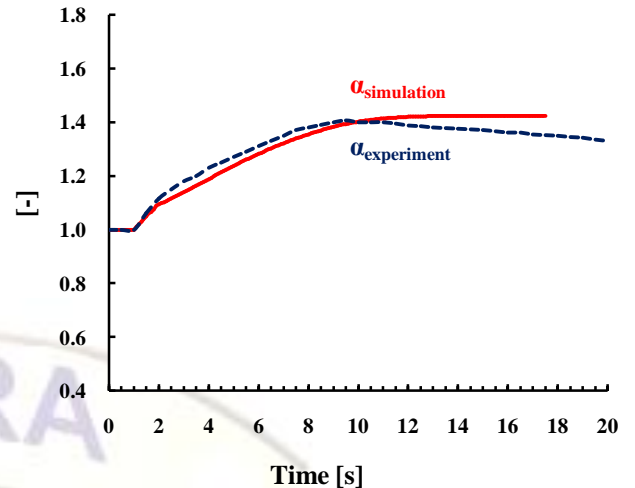
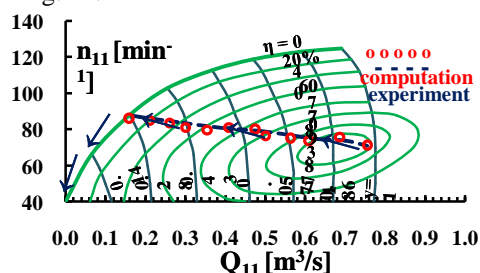


Fig. 13. Results of the computation and experimental data for  $\alpha$  (runaway) (Case B)

Fig. 14. Operating point trajectory in the plan  $Q_{11}(n_{11})$  during unit load rejection (Case B)

### III.2. Case study C: Hydroelectric power plant with surge tank

This case study focuses on a hydropower plant model consisting of the following components: upstream reservoir, gallery, throttled surge tank, penstock, valve, units (two 40 MW vertical Francis turbines and generators) and downstream reservoir (Fig.15). Technical characteristics of the HPP are presented in table 4.

The following transient computation scenarios of hydroelectric power plant are analyzed:  
**Scenario 1:** load rejection (simultaneously) of the Unit 1# (40MW) and Unit 2# (40MW) and  
**Scenario 2:** load rejection of the Unit 1# (30MW) while Unit 2# is in standby mode.

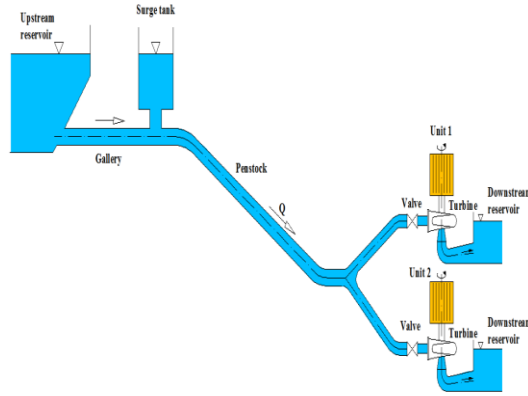


Fig. 15. Layout of the HPP (Case study C)

The guide vanes closing law ( $y$ ) after load rejection is shown in Fig. 16.

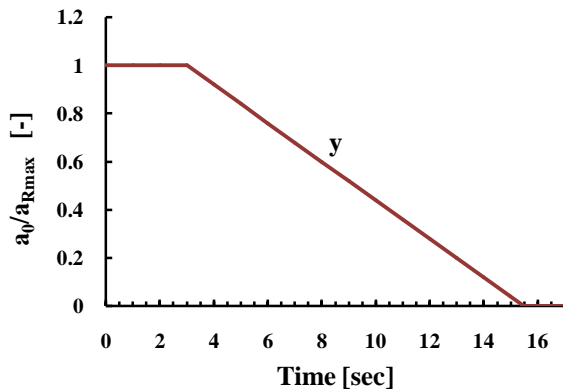


Fig. 16. Guide vanes closing law after load rejection (Case C)

The results of the numerical simulation and experimental data [9,12] of transient phenomena for scenarios 1 and 2 (Case C), are presented on figures below.

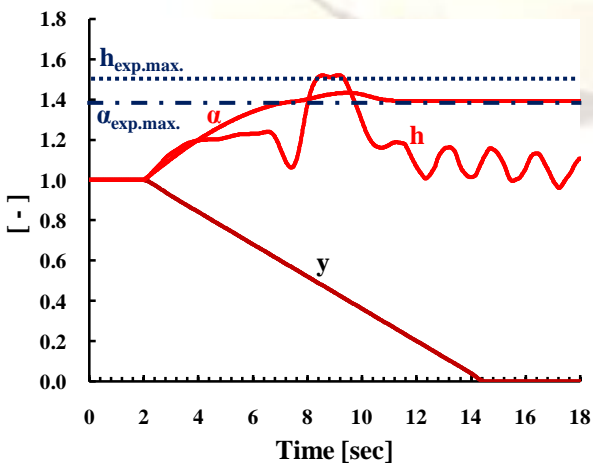


Fig. 17. Results of the computation and experimental data for  $\alpha$  (runaway) and  $h$  (water hammer) for scenario 1 (Case C)

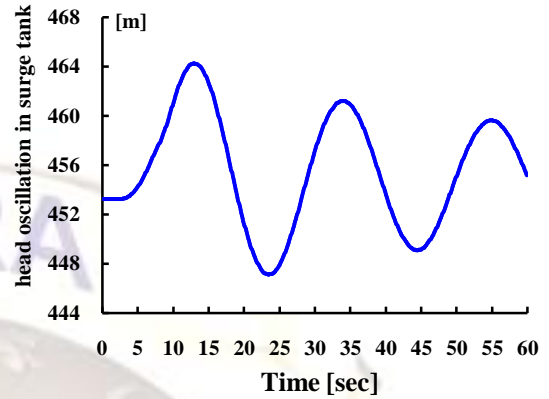


Fig. 18. Result of the computation for head  $z$  (oscillation) in the surge tank (Case C - scenario 1)

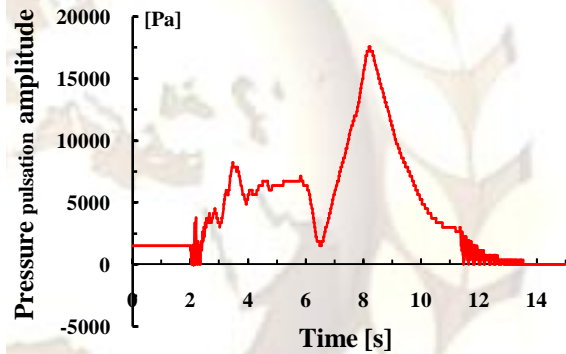


Fig. 19. Result of the computation for draft tube pressure pulsation amplitude (Case C - scenario 1)

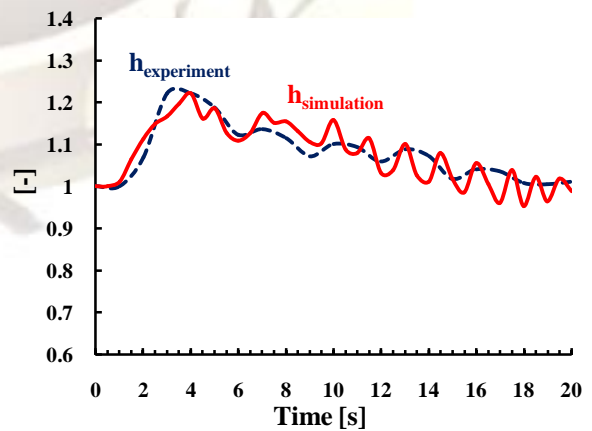


Fig. 20. Results of the computation and experimental data for  $h$  (water hammer) (Case C - scenario 2)

Table 5. The comparison of the results (Case B and

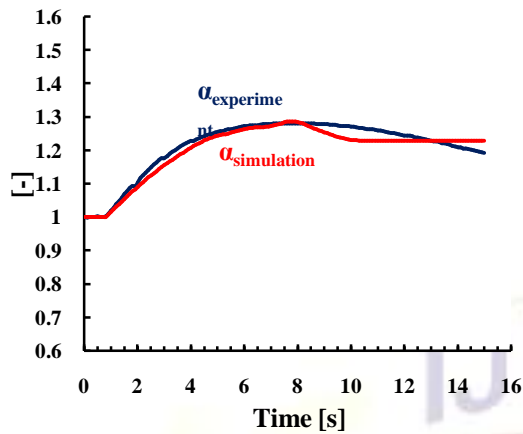


Fig. 21. Results of the computation and experimental data for  $\alpha$  (runaway) (Case C - scenario 2)

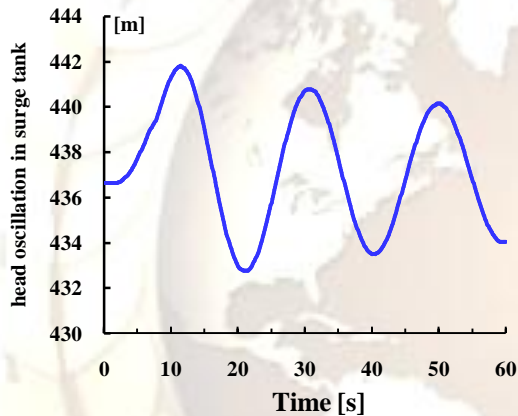


Fig. 22. Result of the computation for head  $z$  (oscillation) in the surge tank (Case C - scenario 2)

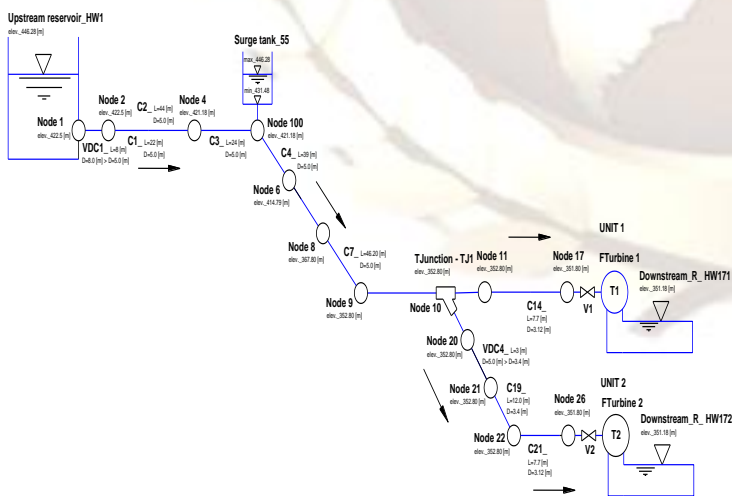


Fig. 24. Numerical model of HPP in WHAMO (Case C)

	Experiment		Computation		Error	
	$\alpha_{max}$ [-]	$h_{max}$ [-]	$\alpha_{max}$ [-]	$h_{max}$ [-]	$\alpha$ [%]	$h_{max}$ [%]
Case B	1.395	1.60	1.410	1.54	1.08	-3.90
Case C-Scenario 1	1.390	1.50	1.430	1.520	2.80	1.40
Case C-Scenario 2	1.285	1.245	1.290	1.230	0.4	1.20

C)

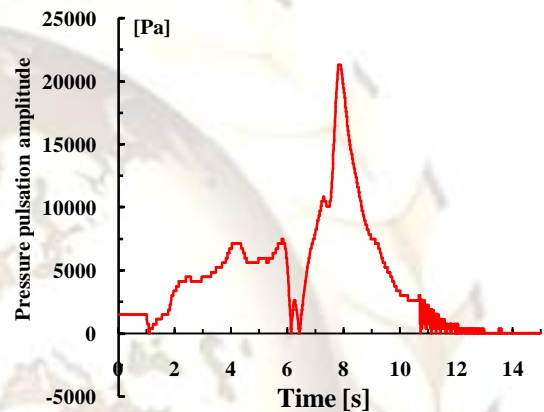


Fig. 23. Result of the computation for draft tube pressure pulsation amplitude (Case C - scenario 2)

The maximum head oscillation in the surge tank for scenarios 1 and 2 is lower compared with maximum allowed value  $H_{Smax}$  (table 4).

Numerical model of the hydroelectric power plant for case C is shown in Fig. 23.

#### IV. VALIDATION OF THE COMPUTATION RESULTS

Validation of the numerical simulations is performed by comparing these results with the obtained experimental data (table 5). After analyzing these values, the following can be concluded:

- the steady state conditions (before the load rejection during generate mode of unit) show very good agreement (the error is 0.1%);
- the time evolution of the heads and rotational speed of the turbine differs for approx. 4%;
- the time of occurrence of the head peaks and max- rotational speed of the turbine differ for approx. 5%;
- the maximum amplitudes (water hammer) at the turbine have a discrepancy of 3.9 percent;



- and finally, the results for the maximum increase of rotational speed of the turbine are in very good agreement (the error is 2.8%).

In general, the comparison of the numerical results and the experimental data (table 5), showed relatively high accuracy of prediction (with discrepancies less than 3.9 percent), which could partially be a result of the measurement accuracy. Errors in the pressure amplitude (water hammer) could also occur due to the differences of the turbine characteristics because of the model/prototype scaling. These characteristics are strongly influenced by the overpressure during load rejection of the unit.

## V. INFLUENTIAL CRITERIA INVESTIGATION OF THE GUARANTEED CONTROL VALUES

All parts of the turbines (spiral case, stator ring, stay vanes, runner, etc.) should be designed in a manner, to be able to withstand all dynamic loads initiated from transient phenomena during off-design operating conditions (water hammer, runaway, vibration, etc.). The values of allowed increase of the pressure (water hammer) and allowed increase of the rotational speed (runaway) are limited with so-called guaranteed control values of the HPP.

One of the main criteria which directly affect the guaranteed control values is the guide vanes closing time of the turbine. Therefore, it is necessary to define the guide vanes' minimum closing time, so that the maximum value of the pressure in the water passage parts and the maximum value of the turbine's rotational speed be within permissible limits i.e. not exceed the guaranteed control values.

To evaluate the influence of the guide vanes' closing time on the guaranteed control values, it's necessary to perform series of computations for different values of the guide vanes' closing time. For this purpose, computations for simultaneous load rejection of the Unit 1 and 2 (case C) during rigorous critical conditions (catastrophic case) are performed and shown in Fig.25. In this computation the guide vanes closing time in all cases is linearly.

Based on the adopted (designed) control values, the required (optimal) guide vanes closing time can be determined (according Fig.25). This time is actually a shortest possible guide vanes closing time!

For example (see Fig.24), if the guide vanes closing time is 10 [s] (linearly closing) then the increase of the head (water hammer) at the turbine is 63% higher compared to the hydrostatic head  $H_0$  ( $h_{max}=1.63$ ), while the increase of the turbine rotational speed (runaway) is 52% higher ( $\alpha_{max}=1.52$ ) compared to the rated value of the rotational speed ( $n_R$ ). These values for the increase the pressure and rotational speed must be (limited) smaller than the guarantee control values ( $h_{max}<h_{guar.}$ ,

$\alpha_{max}<\alpha_{guar.}$ ). Thus, shortest possible guide vanes closing time can be determined.

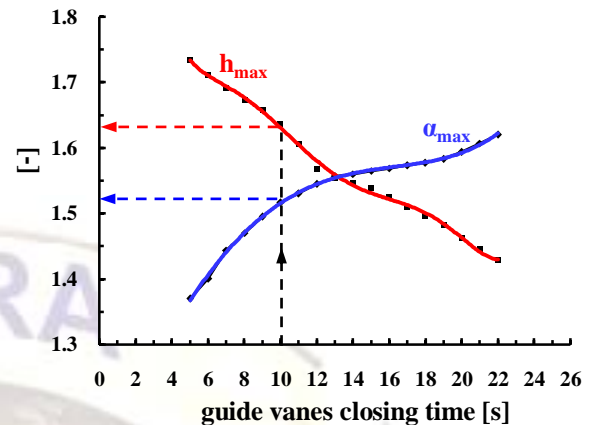


Fig. 25. Non-dimensional pressure increase and rotational speed of the turbine depending of guide vanes closing time

## VI. CONCLUSION

This paper presents numerical and experimental investigation of the transient phenomena in hydroelectric power plants during off-design operating conditions. Different hydraulic configurations during several transient scenarios are produced. The validation of the numerical modeling of transient phenomena is performed by comparison with experimental data. This comparison showed that improved computer methods represent a reliable tool (errors less than 4 percent) and enable detailed analysis of the transient phenomena of HPP during off-design operating conditions.

It has also been concluded that the used numerical models are appropriate for transient analysis of similar hydropower plants and this would reduce the number of the necessary experimental runs in the future. This is particularly important having in mind that such experiments are very hard to organize, require a lot of precaution measures and are costing time and resources the energy producer.

The performed computations will contribute to a much more accurately determination of the following parameters in the design of new HPPs: guide vane closing law after load rejection and normal closing/opening law, accurately determine the increase of the pressure (water hammer), increase the rotational speed (runaway) and draft tube pressure pulsations amplitude at off-design conditions, and accurately determine the rotational inertia characteristics of the units.

Thus, the accurate numerical modeling greatly increases safety and reliability in the design and construction of new power plants, especially those with more complex hydraulic configuration.



## VII. NOMENCLATURE

$a_0$ [mm]	absolute opening of guide vanes
$A$ [m <sup>2</sup> ]	cross section
$a$ [m/s]	wave speed
$C$ [m <sup>2</sup> ]	cavity compliance
$c_Q$ [-]	valve discharge coefficient
$Cr$ [-]	Lewy-Courant number
$D$ [m]	diameter
$E$ [N/m <sup>2</sup> ]	young's modulus of the pipe wall material
$g$ [m/s <sup>2</sup> ]	gravity [m/s <sup>2</sup> ]
$y$ [-]	guide vane opening non-dimensional characteristic
$h$ [-]	piezometric head non-dimensional characteristic, head loss
$H$ [m]	piezometric head
$J$ [kgm <sup>2</sup> ]	mechanical inertia of turbine and generator
$K$ [N/m <sup>2</sup> ]	bulk modulus of the liquid
$k$ [-]	hydraulic loss coefficient
$kt$ [-]	damping coefficient
$k_Q$ [-]	turbine discharge coefficient
$L$ [m]	length
$M_{11}$ [-]	torque factor
$M$ [Nm]	torque
$n$ [min <sup>-1</sup> ]	runner speed (rpm), number of pipe segment
$n_{11}$ [-]	speed factor
$p$ [Pa]	pressure
$P$ [W]	power
$Q$ [m <sup>3</sup> /s]	discharge
$Q_{11}$ [-]	discharge factor
$T$ [s]	period of oscillation
$t$ [sec]	time
$V$ [m <sup>3</sup> ]	volume
$x$ [m]	length
$Z$ [m]	amplitude oscillation
$z$ [m]	head
$\alpha$ [-]	runner speed non-dimensional characteristic
$\delta$ [m]	thickness of the pipe wall
$\Delta x$ [-]	elementary length
$\Delta t$ [-]	time step iteration
$\eta_T$ [-]	turbine efficiency
$\lambda$ [-]	friction factor (Darcy-Weisbach)
$\rho$ [kg/m <sup>3</sup> ]	water density
$\omega$ [rad/sec]	rotating speed
$\tau$ [-]	valve opening/closing non-dimensional characteristic
$\chi$ [s]	mass flow gain factor

- [2] E. Benjamin Wylie, Victor L. Streeter "Fluid Transients", University of Michigan, 2001.
- [3] J. Paul Tullis "Hydraulic of pipelines: pumps, valves, cavitation, transients" Utah State University, USA, 1989.
- [4] Charles Jaeger "Fluid Transients in Hydro-Electric Engineering Practise", University of Glasgow, 1977.
- [5] D.S. Shevelev and others., "Hydroelectric power plants" (Russian), Leningrad State University, 1981.
- [6] Robert Fitzgerald, Vicki L. Van Blaricum, "Water Hammer and Mass Oscillation" 3.0 User's Manual, US Army Corps of Engineers, Research Laboratories, 1998.
- [7] Christophe Nicolet "Hydroacoustic modelling and numerical simulation of unsteady operation of hydroelectric systems" A La Faculte Sciences Et Techniques De Lingenieur, Labaratoire de machines hydrauliques, Thesis No 3751, Lausanne 2007
- [8] J. Kotnik and others, "Overload Surge Event in a Pumped-Storage Power Plant" 23rd IAHR Symposium-Yokohoma, October 2006.
- [9] Viktor Iliev "Analysis of the influence of the unsteady phenomena in the intake structures, penstocks and units of the hydro power plants during transient regimes", Master Thesis, Faculty of Mechanical Engineering, Skopje-Macedonia, 2011.
- [10] S. Mario "Pipeline hydro-dynamics" (Croatian), Faculty of Mechanical Engineering and Naval Architecture, Zagreb, 2005.
- [11] Arshenevskii N.N and others, "Experimental investigation of units load rejection" (Russian), Journal MISI No.35, Moscow-Russian, 1991
- [12] Performances Test Codes "Hydraulic Turbines and Pump-Turbines", American Society of Mechanical Engineers, ASME PTC 18-2002.

## REFERENCES

- [1] M. Hanif Chaudry "Applied Hydraulic Transients", British Columbia Hydro and Power Authority Vancouver, Canada, 1979.